PLOS ONE

RESEARCH ARTICLE

Investigating global phase diagrams (GPDs) with reentrant transition behavior

Jude Simons Bayor[1]*, Baohua Teng[2☯], Lingli Wang[2☯]

1 Department of Applied Physics, Faculty of Applied Sciences, University for Development Studies, Navrongo Campus, Tamale, Ghana, **2** Condensed Matter Physics Department, School of Physical Electronics, University of Electronic Science and Technology of China, Chengdu, People's Republic of China

☯ These authors contributed equally to this work.
* sbayor@uds.edu.gh

Abstract

In this paper we calculate the global phase diagrams with the closed-loop behavior for the phase transition of physical systems by means of the transverse field Ising model with nearest neighbor interaction. The 3D graph plotted by the various physical parameters gives a clear appreciation and qualitative understanding of the reentrant phase behavior of the system. Meanwhile the results show the close correlation between experimental phenomena and our theoretical calculation for the closed-loop behavior for the phase transition of the systems.

Citation: Bayor JS, Teng B, Wang L (2018) Investigating global phase diagrams (GPDs) with reentrant transition behavior. PLoS ONE 13(7): e0199459. https://doi.org/10.1371/journal.pone.0199459

Editor: Nikolaos Fytas, Coventry University, UNITED KINGDOM

Received: February 20, 2018

Accepted: June 4, 2018

Published: July 12, 2018

Data Availability Statement: All relevant data are within the paper and its Supporting Information files.

Funding: The authors received no specific funding for this work.

Competing interests: The authors have declared that no competing interests exist.

Introduction

Phase transition phenomena occur frequently in the natural world [1] and they are of special interest in many fields of study [2]. Hence the shapes of the various phase diagrams have been obtained theoretically by various models and they have significantly enhanced the understanding of the underlying physical property changes [3–29]. Campi et al [28], reports that the lattice gas is viewed as having similar perspective to that of simple fluids, which exhibits a reversed U-shaped phase diagram with the critical point at the top. Also, some complex fluids (examples being certain micro emulsions) with short range interactions exhibit U-shaped phase diagram with the critical point at the bottom. This is observed in the mixture of water and oil in the presence of a surfactant [28]. In fact some more exotic phase diagrams for complex fluids have been reported [16]. For example a solution of nicotine in water, has a closed-loop shaped phase diagram with double critical points [8]. These reentrant phenomena are also reported in various order-disorder systems, such as the composite structure system of potassium [30], the mixed-spin Ising ferrimagnet system [31], the transverse Ising nanosystem [32], and the solvent-mediated protein system [33]. Recently Bayor et al [34] studied the reentrant phase behavior and obtained closed looped shapes that are coincident with the phenomena exhibited in some proteins, colloids and complex fluid mixtures.

In order to investigate systematically the phase behavior in binary systems and other physical systems, the concept of the global phase diagram (GPD) is usually introduced. Earliest studies in global phase diagrams can be alluded to Konynenburg and Scot [35] in a seminal paper of 1980 where they introduced a classification of phase behavior. Goldstein et al [36] studied

rather complex, orientationally specific pair interactions, like those found in real systems by determining the model parameters and thus mapping experiments onto the global phase diagrams. Kolafa et al [37] discovered the azeotropic effect in the complete global phase diagrams for two model binary fluid mixtures described by the one-fluid van der Waals and attractive hard sphere equations of state. GPD not only offers an ideal framework for the theoretical understanding of phase transitions, but also provides the basic relation between phase behavior and underlying intermolecular interactions [37]. Meanwhile the global phase diagram has its origin in the studies of the reappearing phases in some complex systems such as binary fluid mixtures, polar substances, ionic systems, polymer solutions or blends. Of specific interest was how the size and shapes of the closed loops varied with various parameters [38].

In this study we will present the latest calculations of the global phase diagrams by means of the transverse field Ising model with nearest neighbor interaction. Here we will aim at obtaining an agreement between the known experimental phenomena and those from our calculated model and seek to reveal general relationships. The 3D-graph plot of the various physical parameters that we present here, will give a clear appreciation and qualitative understanding of the progressive effect of each parameter change. Also, our GPDs presented, will give the futuristic framework for prediction of the mechanism of the transitions in various systems to guide experimental work that have not been carried out. This is based on the close correlation between present experimental results and our theoretical calculation. It will also afford the possibility to obtain phase diagrams and the critical properties of imaginary or hypothetical physical systems. Once the general phase behavior of condensed matter systems is indispensable and of fundamental interest, an in-depth knowledge by way of our global phase diagrams, will make it easier to translate underlying behavior of systems to offer more complete characterization.

Materials and methods

The model

Usually the transverse Ising model can be used to describe the reentrant phase behavior of the phase diagram of complex fluids [20–24], and its Hamiltonian is as follows [20–24,34]

$$H = -\sum_{i} \Omega S_i^x - \sum_{\langle i,j \rangle} J S_i^z S_j^z \tag{1}$$

Where s_i^x and s_i^z are the x- and z-components of a pseudospin-1/2 operator at site i in the lattice, and $\sum_{<i,j>}$ runs over only nearest-neighboring pairs. Ω is the tunneling interaction parameter and J the exchange interaction parameter.

Using the mean-field approximation, the average occupation number or concentration ρ of the site i of the square lattice can be written as [20–24,34]

$$\rho = 1/2 + (\sigma/2\omega_0) \tanh (\omega_0/2k_B T) \tag{2}$$

where $\omega_0^2 = \Omega^2 + \sigma^2$ $\sigma = \sum_i J < S_i^z >$, and $< S_i^z > = \rho - 1/2$

Here the ensemble average of the pseudo-spin $< S_i^z >$ is the order parameter of the system, and can describe the transition of the system from order given as

$$\langle S_i^z \rangle \neq 0 \tag{3}$$

to a disordered state represented as

$$\langle S_i^z \rangle = 0 \tag{4}$$

Usually we use it to calculate the concentration ρ and analyze the transition behaviors for complex fluid systems [28].

It is established from experimental research in complex fluids that a temperature increase in systems may result in the increase of interaction parameter [11–12], while for some crystal materials the interaction parameter shows positive relationship with temperature [18–19]. Hence with the concept of effective exchange interaction and the temperature dependence, Campi and Krivine [28] obtained closed-loop shaped phase diagrams with the Ising model, and described the reentrant phase behavior of complex fluids. Additionally we suppose in the transverse Ising model, that the effective exchange and effective transverse field parameters J and Ω have simple temperature-dependent relations as in Eqs 5 and 6 [34]:

$$J = J_0\left(\frac{T}{T_0}\right)^n \tag{5}$$

$$\Omega = \Omega_0\left(\frac{T}{T_0}\right)^m \tag{6}$$

where T_0 are arbitrary constants. By this therefore, we can calculate the global phase diagrams involving temperature, concentration, and various interaction parameters for the transverse Ising model with effective temperature-dependent parameters.

Discussions

The global phase diagrams

In this section we obtain the global phase diagrams by solving the formulations in section 2. In calculation, the effective parameters J_0, Ω_0 and k_BT are reduced by k_BT_0, and for simple formalism they are notated still as J_0, Ω_0 and t. In this work we obtain four broad categories of global phase diagrams, show the combined effects of J_0, Ω_0, n and m, and describe their topology and phase transitions in details. For each GPD, any vertical "slice" through the section of the global phase diagram represents the phase diagram for a system with particular values of J_0, Ω_0, m or n strength.

At first category for which the effective field interaction Ω_0 is fixed, let us show what shape of global phase diagrams can be obtained for the exchange interaction J_0 in a case where exponent values of m and n are modified. Fig 1(A) shows such a result, in this case starting with

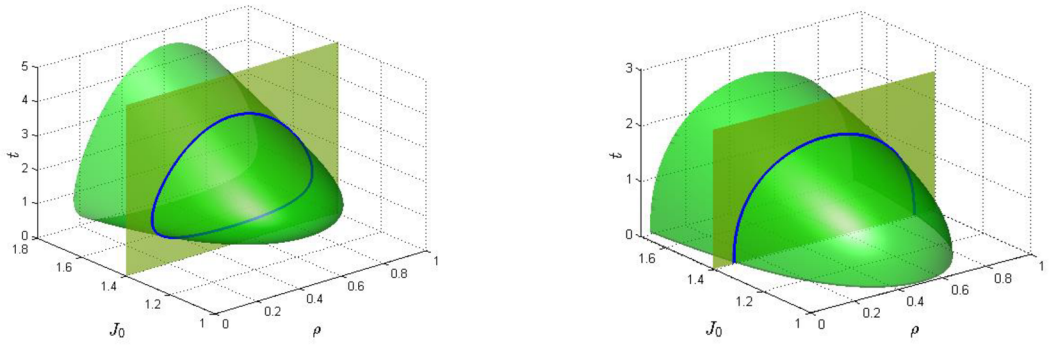

Fig 1. The 3D global phase diagram of the exchange parameter J_0 against temperature t and concentration ρ for $\Omega_0 = 1.10$ and for (a) n = 1.5, m = 2.2, and (b) n = 1.0, m = 2.2.

https://doi.org/10.1371/journal.pone.0199459.g001

large values of m (= 2.2) and n (= 1.5). The global phase diagram has the protuberance of a horn or the section of the nose of a jet plane with the bulging tip oriented towards lower J_0 value and the open end lies towards higher J_0 value. Below a value about $J_0 = 1.15$, the system is completely disordered under all changes in concentration and temperature. However, at a value of just about 1.15, the system shows a coincident double critical point at lower temperature. At this point the system is thus largely disordered for most temperature ranges. Above $J_0 = 1.15$, the egg shaped, closed-loop phase diagram appears with double critical points. An upper critical point corresponds to higher temperatures while its corresponding lower critical point corresponds to lower temperature. As J_0 increases the closed looped shape increases and locus of points becomes broader. Hence the ordered phase becomes more prominent with increase in J_0. This means that the system is largely in the ordered state with increase of J_0. It thus portrays a system with reappearing phases. This phase diagram is coincident with those obtained in our previous work for proteins, colloids and complex fluid mixtures [34]. Typical condensed matter systems that can display this reentrant phase topology include: binary gases, microemulsions, gels, liquid crystals, ferroelectrics granular superconductors, organometallic compounds, etc. [16].

Fig 1(B) shows how the global phase diagram of the effective exchange interaction J_0 varies with temperature and concentrations of the system and on the sensitivity of its exponent n (as it is lowered to n = 1). The global phase diagram is duck-billed shaped. Here the cross sectional phase diagram shows the standard dome shape. As J_0 decreases, this dome shape becomes less pitched and the temperature at which order-disorder transitions occur is lowered for any given concentration. For lower J_0 values, the system is at ordered state at lower temperature and disordered state at higher temperature. At higher J_0 value the system is at ordered state for a large range of temperature. This phase diagram is reversed U-shaped coincident with some usual ferromagnetic systems. This diagram shows that the transitions are sensitively dependent on exponent n, with the loss of reappearing phase property and the system being in ordered state at low temperatures. These systems are ordered at low temperature and disordered at high temperature as the critical temperature typically increases with exchange interaction J_0. This situation corresponds to the usual phase diagram of the TIM with effective temperature-independent parameters [34].

Fig 2 shows the category of global phase diagrams for which we examine the effect of the exponent n on the phase transition of the system and it shows the sensitivity of the effective transverse field Ω_0. The GPD is vuvuzela shaped or can be viewed laterally as having the shape of an hourglass with two distinct phase ranges. While changing J_0, Ω_0, and m, various hourglass shapes are obtainable, some separated at the neck by a gap. The neck (or connection) of the two cone parts as well as the smaller cone are oriented towards lower n while the larger cone is oriented towards higher n. Hence for lower values of n, the system is predominantly at the disordered state at high temperatures and at intermediate temperatures it becomes ordered and for low temperatures it is disordered. The phase diagram is therefore that of a closed looped shape and it shows the characteristics of reappearing phases of the system. The range of concentrations for this phase transition process is very small and thus tapers off and narrows as n increases till at an intermediate point where it again regenerates the closed loop shape. In this part, the phase diagram transcends over a wider range of concentration of the system. Hence at lager values of n, the ordered phase gains some relative prominence in the phase diagram and the reentrant phase behavior with egg-shaped close loop profile is indicative here.

Fig 3(A) shows the how the effective transverse field Ω_0 affects the phase diagram of the system. The GPD has the protuberance of the nose of a jet plane. The cross-section phase diagram is dome shaped with the nose oriented towards higher values of Ω_0 and tapers off. Hence, for high values of Ω_0, the system is predominantly at the disordered state for a large range of

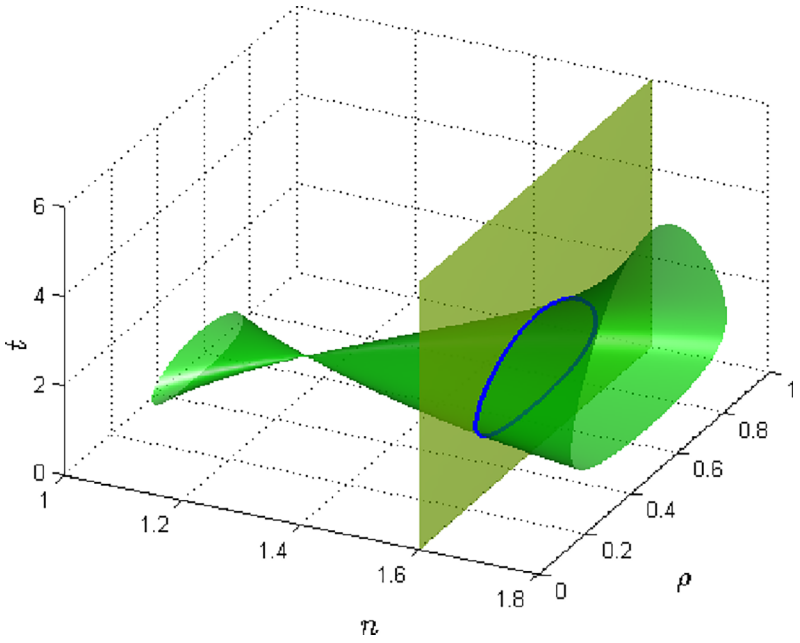

Fig 2. The 3D global phase diagram of the exponent n against temperature *t* and concentration *ρ* for fixed values of $J_0 = 1.10$, $\Omega_0 = 1.11$, m = 2.2.

https://doi.org/10.1371/journal.pone.0199459.g002

higher temperatures while the ordered state transition occurs at a narrow range of low temperature. As Ω_0 gets smaller, the ordered state region gets bigger. So with lower Ω_0, the system is at the ordered state for a progressively wider range of lower temperatures and over wider concentrations as well. This phase diagram is reverse U-shaped and is coincident with usual order-disorder systems. Thus, this parameter has the effect of making the system lose its reappearing phase property.

Fig 3(B) is the GPD showing how the exponents n and m sensitively affect the phase transition diagrams of the system. For the larger values of exponents n and m, the GPD also has the shape of the nose of the jet plane, but the associated phase diagram is closed looped shaped.

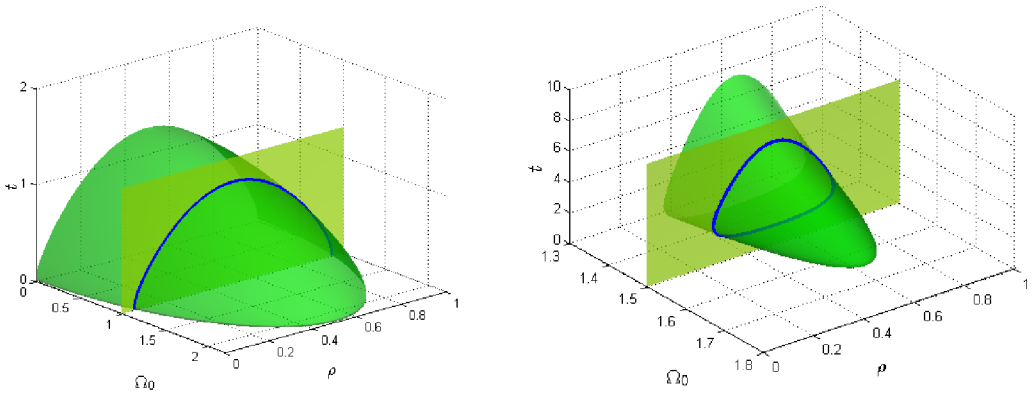

(a) **(b)**

Fig 3. The 3D global phase diagram of the transverse field parameter Ω_0 against temperature *t* and concentration *ρ* for $J_0 = 1.10$ and for (a) n = 0.6, m = 0.6, and (b) n = 1.6, m = 1.8.

https://doi.org/10.1371/journal.pone.0199459.g003

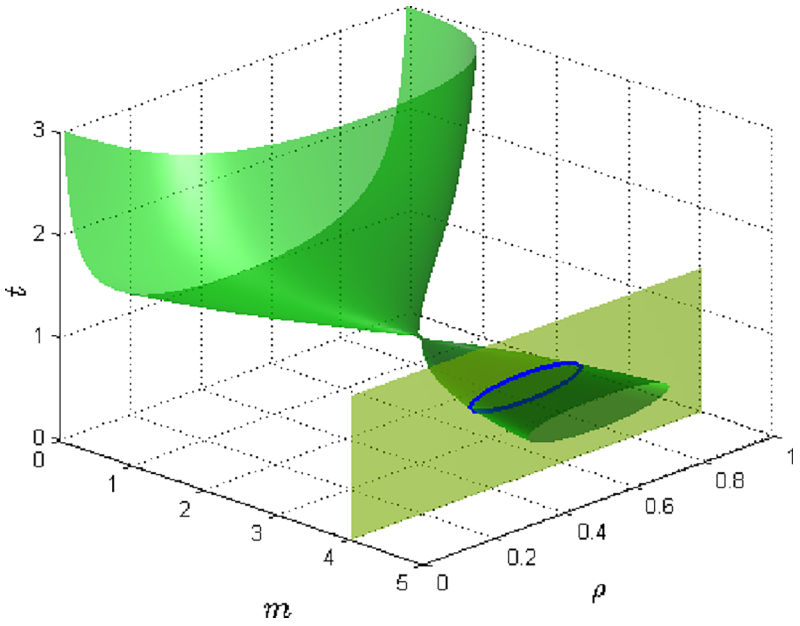

Fig 4. The 3D global phase diagram of the exponent m against temperature *t* and concentration *ρ* for fixed values of $J_0 = 1.25$,n = 1.6,$\Omega_0 = 1.8$.

https://doi.org/10.1371/journal.pone.0199459.g004

For high values of Ω_0 the system is completely at the disordered but as Ω_0 reduces the ordered phase appears and the phenomenon of reappearing phase predominates. Hence the closed loop phase gets bigger and broader over temperature and concentration ranges as Ω_0 decreases. As Ω_0 gets lower, the system is at the ordered state at higher temperatures and largely at disordered state at lower temperatures.

Fig 4 is the category of global phase diagrams showing the effect of the exponent m at varying concentrations and temperatures on the phase transition for systems of given J_0, n, and Ω_0. This diagram shows somewhat two part disjointed global phase diagrams. These two distinct phase ranges that can be separated by a gap when J_0, n, and Ω_0 are changed. As m increases, the diagram shows two quite distinct transition phase characteristics. For low values of m, the system is predominantly at the ordered state at high temperatures and is at disordered at low temperatures. For low m, phase transition process occurs across the large range of concentration from 0 to 1. The phase diagram here is U-shaped. For intermediate values of m, the system is predominantly at the disordered state but has a coincident critical point where it is in ordered state. Hence the phase diagram contracts from oval O-shaped to a point which is described as the double critical point. It thus shows some semblance of reentrant behavior. For high values of m, the system is at disordered state at high temperatures, and is at ordered state at intermediate temperatures, and finally at disordered state at low temperatures. The phase diagram for this section has closed looped shapes varying from that of regular O-shaped to an oblong O-shape as m increases. These shapes are quite exotic in form. Thus, the phenomenon of reappearing phases for this system is favored when m is high. But the spread of concentration ρ of the system for which the process takes place is smaller for high values of m.

Conclusions

This paper provides a theoretical model for accurately obtaining a topological phase transition sequel with closed looped phase behaviors, commonly associated with some binary fluids in

particular, and for other exotic shapes of phase transition phenomena. By using the transverse Ising model and the supposed exponent dependent relations of the effective interaction parameters on temperature, the 3D global phase diagrams were obtained by the mean-field approximation. Cross sections of these global phase diagrams reveal the snap line phase diagrams for systems at the given concentration. Hence four distinct classifications of systems were encountered. These include the phase diagrams of the egg-shaped closed loops, U-shapes, reversed U-shapes and other exotic topologies commonly observed in experiments.

The numerical calculations indicate that the global phase diagrams depend sensitively and dramatically on the exponents n and m, and the strength of effective interaction parameters J_0 and Ω_0. Hence parameter modifications of J_0 and Ω_0 change the features of the global phase diagrams between ordered and disordered states exhibiting the reentrant phase behaviors.

Hopefully these results as well as the theoretical techniques can greatly provide useful information for understanding experimental observations.

Supporting information

S1 Text. This is the Matlab code for the Monte Carlo simulation used.
(DOCX)

Author Contributions

Conceptualization: Jude Simons Bayor.

Data curation: Jude Simons Bayor.

Formal analysis: Jude Simons Bayor.

Investigation: Jude Simons Bayor.

Methodology: Baohua Teng.

Project administration: Lingli Wang.

Software: Lingli Wang.

Supervision: Baohua Teng.

Visualization: Lingli Wang.

Writing – original draft: Jude Simons Bayor.

Writing – review & editing: Jude Simons Bayor.

References

1. Gulminelli F. EOS and phase transition: Nuclei to stars. Ecole Joliot-Curie (30 years) "Physics at the femtometer scale", Dec 2010, La Colle sur Loup, France. 2011, Ecole-Joliot Curie 2011 proceedings. <in2p-00623348>
2. Mouritsen OG. Computer Studies of Phase Transitions and Critical Phenomena. 1st ed. New York Tokyo: Springer-Verlag Berlin Heidelberg; 1984 . . .
3. Murata K and Tanaka H. Supercooled liquids: Clearing the water. Nature Mater.; 2012; 11: 364.
4. Dong R and Hao J. Complex fluids of poly (oxyethylene) monoalkyl ether nonionic surfactants. Chem. Rev. 2010; 110(9): 4978–5022. https://doi.org/10.1021/cr9003743 PMID: 20560665
5. Liu J, Gomez H, Evans JA, Hughes TJR. and Landis CMJ. Functional entropy variables: A ne methodology for deriving thermodynamically consistent algorithms for complex fluids with particular reference to the isothermal Navier-Stokes-Korteweg equations. Comput. Phys. 2013; 248: 47–86.
6. Laurati M, Gambi CMC, Giordano R, Baglioni P, and Teixeira J. Small-Angle Neutron scattering of mixed ionic Perfluoropolyether Micellar Solutions. The Jounal of Phys. Chem. B.: 2010; 114: () 3855.

7. Reinhardt A, Williamson AJ, Doye JPK, Carrete J, Varela LM, and Louis AA. Re-entrant phase behavior for systems with competition between phase separation and self-assembly. The Journal of Chemical Physics.2011; 134:10) 104905.
8. Davies NSA. and Gillard RD. The solubility loop of nicotine:water. Transition Metal Chemistry.2000; 25 (6): 628–629.
9. Walker JS. and Vause CA. Reappearing Phases.ScientificAmerican. 1987; 256(5): 98–105i.
10. Moelbert S and De Los Rios P. Hydrophobic interaction model for upper and lower critical solution temperatures. Macromolecules. 2003; 36: 5845
11. Chen SH, Rouch J, Sciortino F, and Tartaglia Chen P. Static and dynamic properties of water-in-oil microemulsions near the critical and percolation points. Journal of Physics: Condensed Matter. 1994; 6 (50): 10855.
12. Davies LA, Jackson G, and Rull LF. Closed-loop phase equilibria of a symmetrical associating mixture of square-well molecules examined by Gibbs ensemble Monte Carlo simulation. Phys. Rev. Lett. 1999; 82: () 5285.
13. Hudson CSZ. The Reversible Solubility of Nicotine in Water. Z. Phys. Chem. 1904; 47: 113
14. Lang JC and Morgan RD. Nonionic surfactant mixtures. I. Phase equilibria in $C_{10}E_4$–H_2O and closed-loop coexistence. J. Chem. Phys.1980; 73: () 5849.
15. Nord FF, Bier M, and Timasheff SN. Investigations on Proteins and Polymers. IV.[1] Critical Phenomena in Polyvinyl Alcohol-Acetate Copolymer Solutions. J. Am. Chem. Soc.1951; 73: 289.
16. Narayanan T and Kumar A. Reentrant phase transitions in multicomponent liquid mixtures. Phys. Rep. 1994; 249(3): 135–218.
17. Dias CL. Unifying microscopic mechanism for pressure and cold denaturations of proteins. Phys. Rev. Lett. 2012; 109(4): 048104. https://doi.org/10.1103/PhysRevLett.109.048104 PMID: 23006112
18. Xavier MM Jr, Cabral FAO., de Araújo JH, Dumelow T, and Coelho AA. Reentrant spin glass behavior in polycrystalline $La_{0.7}Sr_{0.3}Mn_{1-X}Fe_XO_3$. Mat. Res.2004: 7(4): 355
19. McCallum RW, Fisher IR., Anderson NE, Canfield PC, Kramer MJ., and Dennis KW. Reentrant behavior in the temperature dependence of metamagnetic transitions in single crystal Nd/sub 6/Fe/sub 13-x/Al/sub 1+x/.IEEE Trans. Magn.2001; 37(4): 2147–2149.
20. Wang CL., Zhong WL., and Zhang PL. The Curie temperature of ultra-thin ferroelectric films. J. Phys.: Condens. Matter,. 1992; 4(19): 4743.
21. Kaneyoshi T. Phase diagram of Ising thin films with decorated surfaces; decoupling approximation. Physica A: Statistical Mechanics and its applications. 2001; 293(1–2): 200–214
22. Wesselinowa JM. Properties of ferroelectric thin films with a first-order phase transitions. Solid State Comm. 2002; 121 (2–3) 89.
23. Saber A, Russo SLo, Mattei G, and Mattoni A. Ferromagnetic transitions of a spin-one Ising film in a surface and bulk transverse fields.JMMM. 2002; 251(2) 129
24. Teng BH. and Sy HK. Green's function investigation of transition properties of the transverse Ising model. Phys. Rev. B. 2004; 70:104115
25. Poland D and Scheraga HA. Theory of helix-coil transitions in biopolymers. New York: Academic Press; 1970.
26. Badasyan A, Tonoyan S, Giacometti A, Podgornik R, Parsegian VA, Mamasakhlisov Y et al. Osmotic Pressure Induced Coupling between Cooperativity and Stability of a Helix-Coil Transition. Phys. Rev. Lett. 2012; 109: 068101. https://doi.org/10.1103/PhysRevLett.109.068101 PMID: 23006307
27. Zamparo M and Pelizzola A. Kinetics of the Wako-Saito-Munoz-Eaton model of protein folding. Phys. Rev. Lett. 2006; 97: 068106. https://doi.org/10.1103/PhysRevLett.97.068106 PMID: 17026210
28. Campi X and Krivine H. Ising model with temperature-dependent interactions.Europhys. Lett. 2004; 66 (4): 527.
29. Likos CN. Effective interactions in soft condensed matter physics. Phys. Rep.2001; 348(4–5) 267.
30. Lundegaard LF., Stinton GW., Zelazny M, Guillaume CL, Proctor JE, Loa IE. et al. Phys. Rev. B Observation of a reentrant phase transition in incommensurate potassium. 2013; 88(5): 054106.
31. Strečka J, Ekiz C. Reentrant phase transitions and multicompensation points in the mixed-spin Ising ferrimagnet on a decorated Bethe latticePhysica A 2012; 391(20): 4763.
32. Kaneyoshi T. Reentrant phenomena in a transverse Ising nanowire (or nanotube) with a diluted surface: Effects of interlayer coupling at the surface. Journal of Magnetism and Maggnetic Materials. 2013; 339:151.
33. Möller J, Grobelny S, Schulze J, Bieder S, Steffen A, Erlkamp M, et al. Reentrant liquid-liquid phase separation in protein solutions at elevated hydrostatic pressures. Phys. Rev. Lett. 2014; 112(2):028101 https://doi.org/10.1103/PhysRevLett.112.028101 PMID: 24484044

34. Bayor JS, Teng BH, Zhou S, Zhou L, Chen X, Wu M, et al. The possible phase diagrams for the transverse Ising model with temperature dependent parameters. Chem. Phys. Lett. 2014; 605–606:121–125.

35. van Konynenburg PH, and Scott RL. Critical lines and phase equilibria in binary van der Waals mixtures. Philos. Trans. R. Soc. London A1980; 298: 495–50.

36. Goldstein RE and Walker JS.Theory of multiple phase separations in binary mixtures: Phase diagrams, thermodynamic properties, and comparisons with experiments J. Chem. Phys. 1983; 78:1492.

37. Kolafa J, Nezbeda I, Pavlīcek J, and Smith WR. Global phase diagrams of model and real binary fluid mixtures: Lorentz–Berthelot mixture of attractive hard spheres. Fluid Phase Equilibria. 1998; 146(1–2): 103–121.

38. Walker JS and Vause CA. Theory of closed-loop phase diagrams in binary fluid mixtures. Physics Letters A. 1980; 79(5–6):421–424.